Desalination and Water Treatment
www.deswater.com

doi: 10.1080/19443994.2014.911708

55 (2015) 132–141
June

Taylor & Francis
Taylor & Francis Group

2,4-Dichlorophenoxyacetic acid adsorption onto coconut shell-activated carbon: isotherm and kinetic modeling

V.O. Njoku[a,b], M. Asif[c], B.H. Hameed[a,*]

[a]*School of Chemical Engineering, Engineering Campus, Universiti Sains Malaysia, Nibong Tebal 14300, Penang, Malaysia, Tel. +60 45996422; Fax: +60 45941013; email: chbassim@eng.usm.my*
[b]*Faculty of Science, Department of Chemistry, Imo State University, P.M.B. 2000, Owerri, Nigeria*
[c]*Chemical Engineering Department, College of Engineering, King Saud University, P.O. Box 800, Riyadh 11421, Saudi Arabia*

Received 14 January 2014; Accepted 30 March 2014

ABSTRACT

The removal of 2,4-dichlorophenoxyacetic acid (2,4-D) from aqueous solution by coconut shell-activated carbon (CSAC) was studied adopting batch adsorption techniques. The effect of contact time, initial concentration of 2,4-D, and pH was investigated. From the kinetic data, 8 h was considered as the equilibrium time for determining adsorption isotherms. Adsorption data were fitted to the Langmuir, Freundlich, Temkin, and the new Brouers–Sotolongo (BS) adsorption isotherms. Results showed that the BS isotherm model best described the adsorption process and the BS maximum adsorption capacity determined was 368.0 mg/g at 30°C. The Lagergren pseudo-first-order, Ho pseudo-second-order, Elovich, and the new Avrami models were applied to fit the kinetic results and it was found that the Avrami model was most suitable. The adsorption decreased with increasing pH, in the pH range 3–9, due to increased repulsion between 2,4-D molecules and CSAC surface. The results suggest that CSAC is effective as adsorbent for 2,4-D removal from water.

Keywords: 2,4-D; Adsorption isotherms; Kinetic modeling; Pesticides; Water treatment

1. Introduction

Water pollution by pesticides, especially the organochlorines, has generated public concern throughout the world in the last few decades because of their toxicity and persistence in the environment, being mostly non-biodegradable [1]. These compounds are dangerous to human health and the environment even at low concentrations [2]. 2,4-Dichlorophenoxyacetic acid (2,4-D), an organochlorine and an anionic phenoxy herbicide, is widely applied in the control of broad leaf weeds and grasses in crop plantations and lawns, because of its low cost, good selectivity, and effectiveness [3]. Since 2,4-D is used in the open environment, its residues easily find their way into water resources, thereby contaminating them [4].

Consequently, several techniques have been developed for the removal of pollutants from water. Most of these techniques adopt a combination of physical, chemical, and biological processes which include photo-oxidation, chemical coagulation, sedimentation, filtration, disinfection, and adsorption. Nevertheless, adsorption is one of the most efficient methods for removal of pollutants from water offering many economical, technological, and ecological advantages [5–10]. A number of adsorbents have been used for

---

*Corresponding author.

the removal of 2,4-D including fertilizer and steel industry wastes, organo-palygorskite, bituminous shale, and calcined hydrotalcite [11–14]. Recently, new materials like metal organic frameworks have been used for the adsorption of 2,4-D and other chloroaromatics even though it is not so attractive for economic reasons [15,16]. Activated carbon has evolved as one of the most favored adsorbents for the removal of pesticides and other pollutants from water and wastewater because of its large surface area, porosity, thermo-stability, low acid/base reactivity, and efficiency even at low concentrations of pollutants [17–20]. Some researchers have demonstrated the use of activated carbon in the removal of pesticides and other pollutants from aqueous phase [21–26], nonetheless, there is relative paucity of literature covering the removal of 2,4-D by activated carbon. Chingombe et al. [27], as well as Salman and Hameed [28] demonstrated the use of commercial activated carbon made from coal-based sources in the removal of 2,4-D from aqueous solutions. A variety of materials have been utilized for the production of activated carbon including wood, sawdust, nutshells, fruit stones, peat, lignite, coal, and petroleum coke [29]. The specific precursor has been shown to have impact on the textural properties and adsorption performance of activated carbon for particular applications [30–32]. Previous studies have shown that the presence of other inorganic salts and organics in water/wastewater reduces the adsorption capacity of the sorbent for the sorbate [32].

In this study, activated carbon prepared from coconut shell-activated carbon (CSAC) was studied for its adsorptive performance in the removal of 2,4-D from aqueous solutions. The activated carbon was characterized by surface area, pore structural features, fourier transform infrared (FTIR) spectroscopy, and scanning electron microscopy (SEM). The effects of contact time, initial concentration of 2,4-D, and initial solution pH were investigated. Langmuir, Freundlich, Temkin, and Brouers–Sotolongo (BS) models were used in fitting equilibrium isotherm data to determine maximum adsorption capacity and nature of adsorption. Kinetic parameters were also obtained to elucidate the adsorption mechanism.

2. Materials and methods

2.1. Adsorbate

Analytical grade 2,4-D of 97% purity was supplied by Sigma–Aldrich (M) Sdn. Bhd., Malaysia and was used as adsorbate as received without further treatment. Distilled water was used in the preparation of all solutions. The physicochemical properties of 2,4-D are listed in Table 1.

2.2. Adsorbent

The adsorbent used in this study is CSAC, produced by steam activation. It was in granular form and was obtained from local market, Malaysia. It was used without further treatment. Some physical and chemical properties of CSAC as provided by the supplier are presented in Table 2.

2.3. Characterization of CSAC

The surface area and pore characteristics of CSAC were measured using a surface area and porosity analyzer (Micromeritics, ASAP 2010, USA), which uses nitrogen adsorption–desorption method at 77 K. The density functional theory model was used to analyze the results. The functional groups present on the surface of the activated carbon were determined using FTIR spectroscopy (Perkin–Elmer, Model 2000 FTIR,

Table 1
Physicochemical properties of 2,4-D

Chemical structure	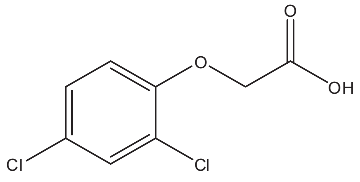
CAS number	94-75-7
Molecular formula	$C_8H_6Cl_2O_3$
Molecular weight (g/mol)	221.04
Melting point (℃)	140.5
Boiling point at 0.4 mm Hg (℃)	160
Solubility in water at 25℃ (mg/L)	900
pK_a	2.8

Table 2
Some physical, chemical, and textural characteristics of CSAC

Form	Granular
Size (mm)	0.045–0.212
Iodine number (mg/g)	1,000
Apparent density (g/cm^3)	0.50
Ball pan hardness (%, minimum)	98
Moisture content (%)	<5
Ash content (%)	<3
BET surface area (m^2/g)	986.2
Mesopore area (m^2/g)	40.25
Micropore area (m^2/g)	945.9
Total pore volume (cm^3/g)	0.54
Average pore diameter (nm)	2.20

USA). The KBr pellet method was adopted for sample handling and the spectrum was run from 4,000 to 400 cm^{-1}. The surface morphology of CSAC was studied by examining the sample under a SEM (Model Supra 50VP-23-57, Germany).

2.4. Adsorption studies

Stock solution of 500 mg/L 2,4-D was prepared by dissolving 515.46 mg of 2,4-D (97% purity) in a 1 L volumetric flask under stirring and making up the volume to the mark using distilled water. Different initial solution concentrations of 50–300 mg/L were prepared by serial dilution of the stock solution. The kinetic and equilibrium studies were undertaken at the pH of 3.5. Batch adsorption studies were performed by shaking 200 mL of the 2,4-D solution of desired concentration with 0.2 g of CSAC. The CSAC dose used is the optimum in the range of initial concentrations of 2,4-D studied and was obtained from preliminary experiments. The water bath shaker was set at temperature 30°C and speed 120 rpm. For the pH studies, the initial pH of the solutions before contact were adjusted to pH 3–11 using 0.1 M HCl and 0.1 M NaOH and 2,4-D initial concentration of 100 mg/L was used. The final concentrations of 2,4-D were measured at predetermined time intervals using a double beam UV/Visible spectrophotometer (Shimadzu, Model UV 1700, Japan) at 283 nm. The 2,4-D uptake at a given time, q_t (mg/g), was calculated using Eq. (1).

$$q_t = \frac{(C_0 - C_t)\,V}{M} \tag{1}$$

where C_0 (mg/L) and C_t (mg/L) are the concentrations of 2,4-D in the liquid phase at the initial and time t, respectively; V (L) the volume of solution treated and M (g) the dry mass of CSAC.

3. Results and discussion

3.1. Characterization of CSAC

The surface area, pore volume, and pore size data for CSAC are also summarized in Table 2. Adsorbent pores can be classified using their pore diameter based on the definition by the International Union of Pure and Applied Chemistry as micropores (<2 nm), mesopores (2–50 nm), and macropores (>50 nm) [33]. The average pore diameter of CSAC was found to be 2.2 nm, indicating mesoporosity. The FTIR spectrum of CSAC is shown in Fig. 1. The peak observed at 3,402 cm^{-1}, is typical of O–H stretching vibration

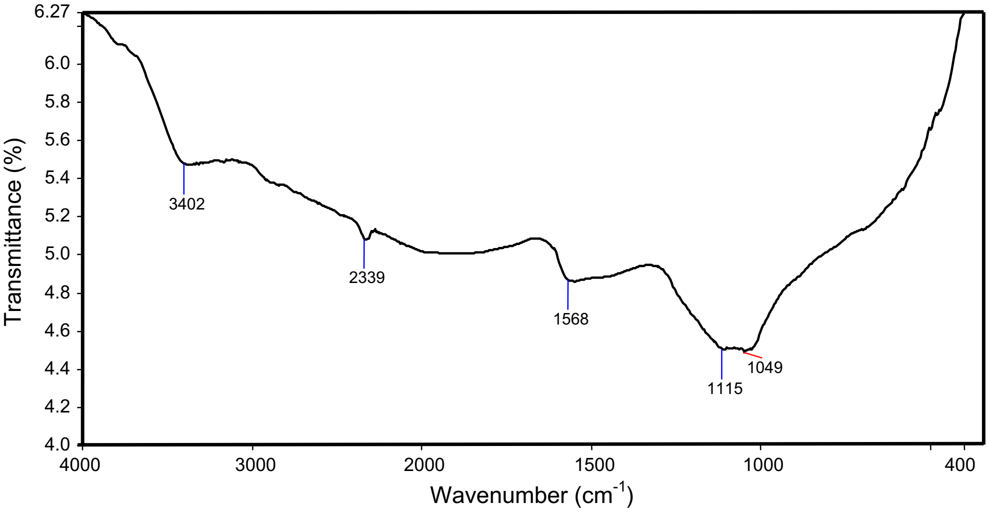

Fig. 1. FTIR spectrum of CSAC.

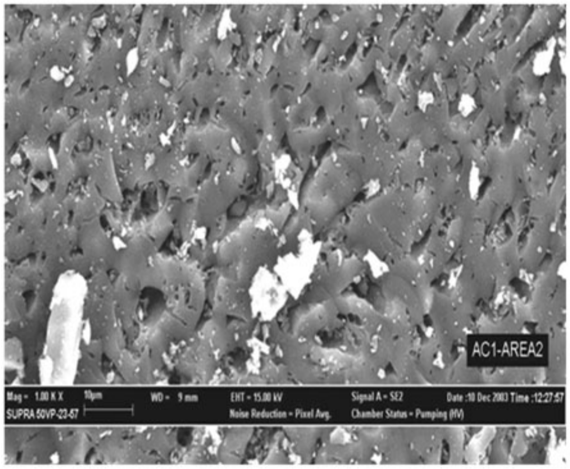

Fig. 2. SEM image of CSAC.

mode of hydroxyl functional group including H bonding [34,35]. The peak at 2,339 cm^{-1} denotes the C≡C stretching vibrations in alkyne groups [17], while the peak at 1,568 cm^{-1} indicates the C=C stretching vibration of aromatic rings [36]. The bands at 1,115 and 1,049 cm^{-1} are assigned to C–OH stretching vibration in secondary and primary alcohols, respectively [37]. On the overall, the significant functional groups identified in the FTIR analysis are hydroxyl, unsaturated bonds of carbon and aromatic groups. The scanning electron micrograph of CSAC at 1,000 magnification is shown in Fig. 2. From the figure, it could be observed that the CSAC surface has well-distributed pores, where 2,4-D molecules could be trapped and adsorbed.

3.2. Effect of contact time and initial concentration of 2,4-D

The effect of contact time and initial concentration of 2,4-D on the adsorption was studied in the 2,4-D initial concentration range 50–300 mg/L. Other conditions used are pH 3.5, CSAC dose 1,000 mg/L, 30°C temperature, and 120 rpm speed. The studies were undertaken at different contact times to establish the equilibrium time. Fig. 3 shows the plots of 2,4-D concentration against contact time for different initial concentrations of 2,4-D. It shows that the concentration of 2,4-D decreases with increase in contact time indicating an increase in adsorption with increase in contact time, until equilibrium is reached at a certain time. The result reveals that the adsorption is fast at the initial stage and becomes slower as it approaches to equilibrium. This could be explained on the basis of availability of vacant sites on the CSAC surface. With increase in contact time, most of the sites become

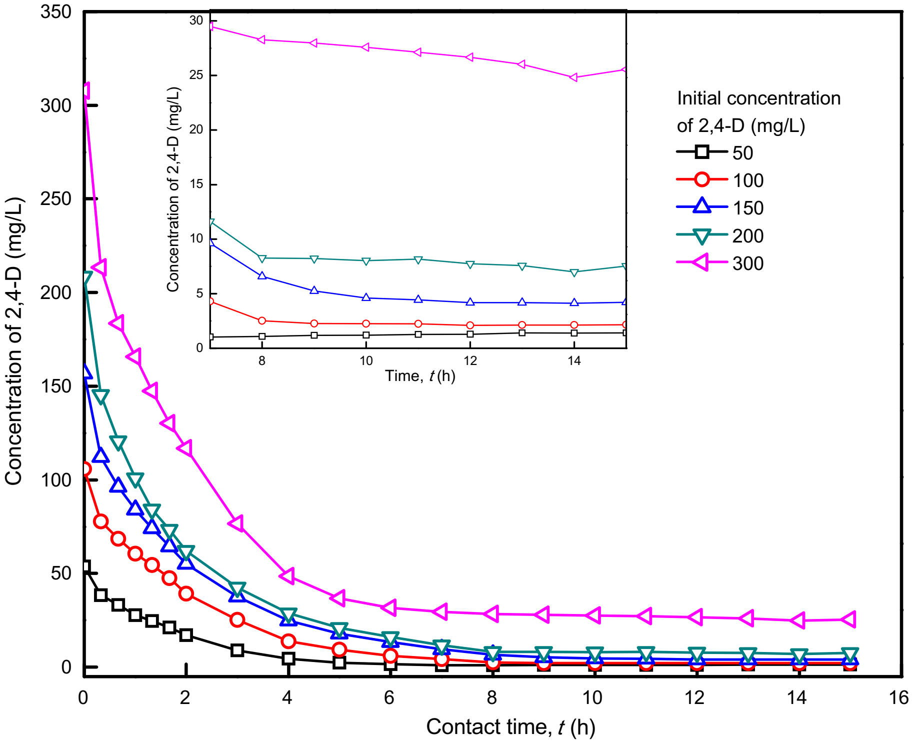

Fig. 3. The effect of contact time on 2,4-D concentration (30°C; agitation speed, 120 rpm; CSAC dose, 1,000 mg/L).

occupied leading to decrease in the number of available sites for adsorption which in turn reduces the adsorption rate. From Fig. 3, it could be seen that equilibrium was attained in 8 h. Therefore, a contact time of 12 h was set for subsequent studies to ensure that equilibrium was attained.

From Fig. 3, it could further be observed that the initial concentration of 2,4-D plays an important role in the adsorption of 2,4-D onto CSAC. The amount of 2,4-D adsorbed on CSAC increased with increase in initial concentration of 2,4-D. This could be attributed to the utilization of all available active sites for adsorption at higher 2,4-D concentration, a larger mass transfer driving force and increased number of collision between 2,4-D molecules and CSAC.

3.3. *Effect of initial solution pH on 2,4-D adsorption*

Solution pH affects the surface charge of the adsorbent and the degree of ionization of the adsorbate and is therefore one of the most important parameters affecting adsorption process in aqueous solutions. The pH studies were undertaken in the pH range 3–11 using 100 mg/L 2,4-D and 1,000 mg/L CSAC dose at 30˚C and 120 rpm. The effect of initial pH on the adsorption of 2,4-D is depicted in Fig. 4. It could be observed that the equilibrium adsorption quantity (uptake) decreased with increasing solution pH from 3 to 9 and showed a slight increase with further increase in pH. This behavior clearly indicates that the adsorption was characterized by interaction between 2,4-D and the CSAC surface. 2,4-D can be dissociated in water solution according to the reaction:

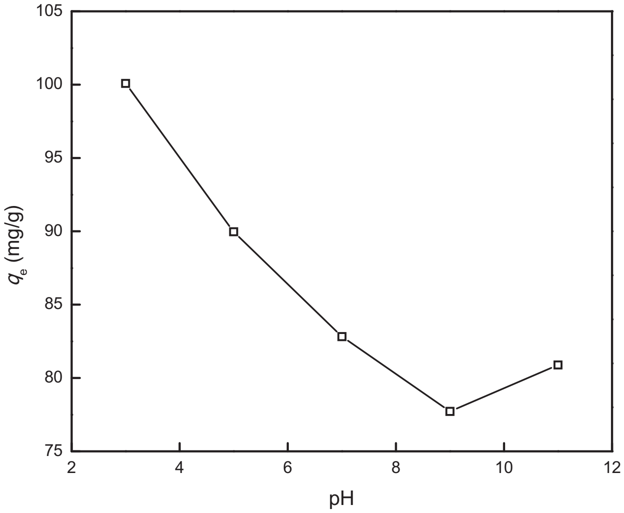

Fig. 4. The effect of solution pH on 2,4-D equilibrium adsorption.

$$2,4\text{-D} + \text{OH}^- \rightarrow 2,4\text{-D}^- \ (\text{deprotonated form}) + \text{H}_2\text{O} \quad (2)$$

The protonated species is dominant when the solution pH is below 2.8 the pK_a of 2,4-D while at higher solution pH, 2,4-D is dissociated and a greater proportion is in the ionized form, 2,4-dichlorophenoxyacetate ion. The main factors influencing the pH profile being the repulsion between the negatively charged hydroxyl functional groups on CSAC surface, as was revealed by the FTIR spectroscopic analysis. This clearly shows the absence of strong chemical interactions and therefore the proposed mechanism of adsorption is physisorption.

Similar observations were reported in some previous studies [11,28]. The increase in 2,4-D uptake at pH higher than 9 could be attributed to precipitation of the adsorbate in strong alkaline media [38].

3.4. *Adsorption isotherms modeling*

Adsorption isotherms are mathematical models that describe the distribution of the adsorbate species between the liquid phase and the solid phase when the adsorption process reaches equilibrium state. The experimental data obtained in this study were fitted to four adsorption isotherms: Langmuir, Freundlich, Temkin, and the new BS models. The Langmuir isotherm model [39] is given by:

$$q_e = \frac{q_m K_L C_e}{1 + K_L C_e} \quad (3)$$

where q_e (mg/g) represents the amount of 2,4-D adsorbed at equilibrium, q_m (mg/g) the maximum monolayer adsorption capacity, C_e (mg/L) the equilibrium concentration of 2,4-D in the liquid phase, and K_L (L/mg) a constant related to the affinity of binding sites. The Langmuir adsorption model assumes that maximum adsorption corresponds to a monolayer saturation of 2,4-D molecules on the CSAC surface, and that no lateral interaction between the 2,4-D molecules exists [40]. The Freundlich isotherm model [41] is based on the assumption of adsorption on heterogeneous surface, whereby the stronger sites are occupied first and the binding strength decreases as more sites are occupied [42] and is given by:

$$q_e = K_F C_e^{1/n} \quad (4)$$

where K_F (L/g), defined as the adsorption or distribution coefficient, is related to the adsorption capacity and therefore a measure of the affinity of the adsorbent for the adsorbate and n is a measure of the adsorption intensity. The value of $1/n$ usually falls in the range 0–1 and gives an indication of the surface heterogeneity of the adsorbent. The more the value tends to 0, the more heterogeneous the adsorbent surface. The Temkin isotherm [43] considers the effects of indirect adsorbate–adsorbate interactions on adsorption isotherm and assumes that heat of adsorption decreases linearly with coverage due to adsorbate–adsorbate interactions. It is commonly expressed by:

$$q_e = \frac{RT}{b_T} \ln(AC_e) \tag{5}$$

where b_T (J/mol) is the Temkin isotherm constant related to the heat of adsorption and is given by $b_T = -\Delta H/q_m$ [44]; A (L/g) a constant corresponding to the maximum binding energy; R (8.314 J/mol K) the universal gas constant, and T (K) the absolute temperature. The BS isotherm [45] is defined by a deformed exponential (Weibull) function and is given by:

$$q_e = q_m(1 - \exp(-K_{BS} C_e^{\alpha})) \tag{6}$$

where the BS constant K_{BS} (L/mg) = K_F/q_m, and the exponent, α (dimensionless) is a measure of the width of the adsorption energy distribution and therefore of the energy heterogeneity of the adsorbent surface.

The equilibrium data for the adsorption of 2,4-D onto CSAC at 30°C were fitted to the four adsorption isotherm models by non-linear regression methods. The non-linear fits of the adsorption equilibrium data for the four isotherm models are shown in Fig. 5, while the isotherm parameter values obtained are listed in Table 3.

The adjusted coefficient of determination (R^2_{adj}), which accounts for the number of variables and sample size in the model, is generally considered superior to the coefficient of determination (R^2), as it corrects the overestimation by R^2 [46]. It is more accurate than R^2 especially when dealing with small samples [47]. The closeness to unity of R^2_{adj} was used to adjudge the goodness-of-fit and applicability of the isotherm models. In addition, the lowest value of the root-mean-squared error (RMSE), also known as standard deviation analyses was utilized in confirming the suitability of the isotherm models in the fitting of adsorption data. The R^2_{adj} and RMSE values obtained from the isotherm models are shown in Table 3. The BS model gives the highest R^2_{adj} and lowest RMSE values, which shows that the adsorption of 2,4-D on CSAC is best represented by the BS model. The good fit obtained with the BS model suggests the existence of a heterogeneous adsorption energy landscape [48]. The BS and Langmuir maximum adsorption capacities obtained at 30°C were 368.0 and 352.3 mg/g, respectively. The Temkin isotherm parameter, b is related to the heat of adsorption, and the positive values obtained for 2,4-D adsorption onto CSAC is indicative of an exothermic process. The Hall separation factor (dimensionless constant), R_L [49] was calculated from the Langmuir parameter, K_L, using Eq. (7):

$$R_L = \frac{1}{1 + K_L C_0} \tag{7}$$

where K_L is the Langmuir parameter defined earlier and C_0 (mg/L) the initial concentration of 2,4-D. The values of R_L obtained could be used in the interpretation of adsorption type as unfavorable ($R_L < 0$ or $R_L > 1$), favorable ($R_L < 1$ or $R_L = 1$ (linear)), and irreversible ($R_L = 0$) [50]. In this study, the R_L values were found to be in the range 0.02–0.11 at 30°C, indicating that the adsorption of 2,4-D onto CSAC is a favorable process.

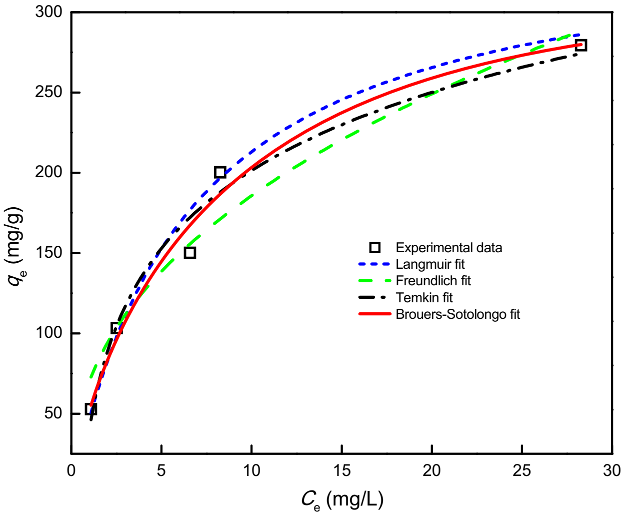

Fig. 5. Adsorption isotherms for 2,4-D adsorption onto CSAC at 30°C.

The Langmuir maximum monolayer adsorption capacity for the adsorption of 2,4-D onto various activated carbon reported by other researchers in literature are summarized in Table 4 [27,28,51]. The results showed that activated carbon prepared from coconut shell, CSAC, exhibited higher maximum monolayer adsorption capacity in the removal of 2,4-D than other activated carbons produced from other sources.

Table 3
Langmuir and Freundlich isotherm model parameters for adsorption of 2,4-D onto CSAC at 30℃

Langmuir				Freundlich				Temkin				Brouers–Sotolongo				
K_L (L/mg)	q_m (mg/g)	R^2_{adj}	RMSE	K_F (L/g)	n	R^2_{adj}	RMSE	A (L/g)	b_T (J/mol)	R^2_{adj}	RMSE	q_m (mg/g)	K_{BS} (L/mg)	α	R^2_{adj}	RMSE
0.15	352.3	0.977	15.08	70.1	2.36	0.941	21.20	1.78	36.0	0.979	14.39	368.0	0.19	0.77	0.985	13.30

Table 4
Comparison of Langmuir adsorption capacities of 2,4-D by various activated carbons under similar conditions

Activated carbon type	Precursor	Adsorption capacity (mg/g)	Reference
Granular activated carbon F400	Coal-based	8.1–10.5	[25]
Modified granular activated carbon F400	Coal-based	11.8–16.3	[25]
Granular activated carbon F300	Coal-based	181.8	[26]
Granular activated carbon	Date stone-based	238.1	[48]
Granular activated carbon	Pumpkin seed hull-based	260.8	[16]
Granular activated carbon	Corncob-based	300.2	[20]
CSAC	Coconut shell-based	352.3	This study

3.5. Adsorption kinetics

To investigate the mechanism of adsorption of 2,4-D onto CSAC, the kinetic data was modeled with the pseudo-first-order, pseudo-second-order, Elovich, and the new Avrami kinetic equations. The Lagergren pseudo-first-order model [52] could be expressed as:

$$q_t = q_e(1 - e^{-k_1 t}) \tag{8}$$

where k_1 (1/h) is the pseudo-first-order rate constant and t (h) the contact time. The Ho pseudo-second-order kinetic model [53] could be represented by:

$$q_t = \frac{q_e^2 k_2 t}{1 + q_e k_2 t} = \frac{h}{1 + q_e k_2 t} \tag{9}$$

where k_2 (g/mg h) is the pseudo-second-order rate constant and h (mg/g h) is regarded as the initial sorption rate, as q_t when t approaches 0, and is given by:

$$h = q_e^2 k_2 t \tag{10}$$

The Elovich equation [54] is given by:

$$q_t = \frac{1}{b}\ln(ab) + \left(\frac{1}{b}\right)\ln t \tag{11}$$

where a (mg/g min) is the initial adsorption rate and b (g/mg) the desorption constant related to the extent of surface coverage and activation energy for chemisorption. The Avrami kinetic equation determines the fractionary kinetic orders and some kinetic parameters reflecting possible changes in the adsorption rates as function of the initial concentration and adsorption time [55]. The Avrami equation [56] is expressed as:

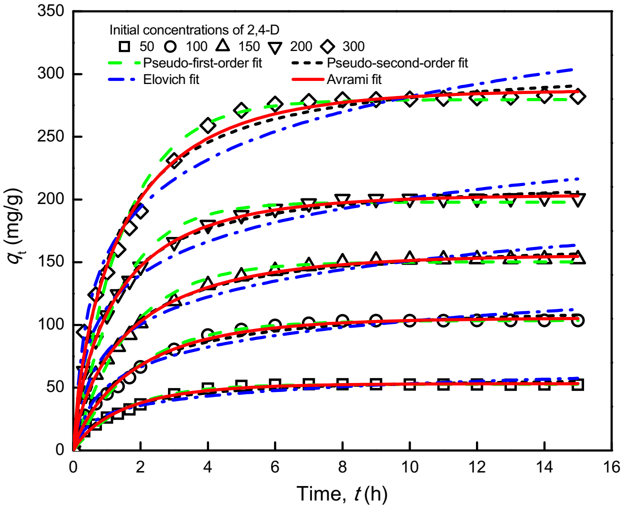

Fig. 6. Kinetic model fitting for the adsorption of 2,4-D on CSAC (30℃; agitation rate, 120 rpm; CSAC dose, 1,000 mg/L).

Table 5
Pseudo-first-order, pseudo-second-order, Elovich, and Avrami rate constants for adsorption of 2,4-D onto CSAC at 30°C

C_0 (mg/L)	$q_{e,exp}$ (mg/g)	Pseudo-first-order				Pseudo-second-order					Elovich				Avrami				
		k_1 (1/h)	q_e (mg/g)	R^2_{adj}	RMSE	k_2 (g/mg h)	h (mg/g h)	q_e (mg/g)	R^2_{adj}	RMSE	a (mg/g h)	b (g/mg)	R^2_{adj}	RMSE	k_{Av} (1/h)	q_e (mg/g)	n_{Av}	R^2_{adj}	RMSE
50	52.5	0.652	52.7	0.990	1.54	0.015	51.7	59.1	0.983	2.07	151.7	0.09	0.951	3.50	0.679	52.5	0.87	0.999	1.68
100	103.6	0.543	103.6	0.990	3.22	0.006	80.1	118.5	0.987	3.65	211.4	0.04	0.966	5.88	0.575	103.6	0.84	0.992	7.50
150	152.5	0.606	150.3	0.984	5.71	0.005	135.6	169.9	0.994	3.61	385.6	0.03	0.979	6.54	0.645	152.5	0.74	0.995	1.30
200	201.0	0.742	197.9	0.985	7.05	0.005	226.1	219.3	0.996	3.60	763.5	0.03	0.973	9.30	0.769	201.6	0.73	0.996	2.20
300	282.1	0.674	279.6	0.978	12.03	0.003	291.0	311.4	0.985	9.96	945.1	0.02	0.965	15.25	0.718	284.1	0.74	0.998	2.22

$$q_t = q_e\{1 - \exp[-k_{Av}(t)^{n_{Av}}]\} \tag{12}$$

where k_{Av} (1/h) is the Avrami kinetic constant and n_{Av} is a constant which can be relational to the adsorption mechanism.

The experimental data were fitted to the four kinetic models by non-linear regression methods as shown in Fig. 6. The kinetic model parameters, R^2_{adj}, and RMSE values obtained are listed in Table 5 and were utilized in confirming the suitability of the models in the fitting of adsorption kinetic data. The R^2_{adj} values for the Avrami model are closest to unity at all initial concentrations of 2,4-D studied and therefore the Avrami model is most suitable for describing the adsorption of 2,4-D on CSAC. The lowest values of the RMSE confirm the applicability of the Avrami model for adsorption of 2,4-D on CSAC. In addition, the q_e values predicted by the Avrami model were closest to experimental values further indicating that the adsorption of 2,4-D onto CSAC follows the Avrami model platform. The best data fit to the Avrami model suggests possible changes of the adsorption mechanism during the adsorption process following multiple kinetic orders that change during the contact of 2,4-D with CSAC [56]. Similar kinetics was observed for the adsorption of methylene blue on activated carbon produced from flamboyant pods [55].

4. Conclusion

The results of this investigation revealed that activated carbon produced from coconut shell (CSAC) has suitable adsorption capacity for the removal of 2,4-D from aqueous solutions. The equilibrium between 2,4-D in solution and on CSAC surface was achieved in 8 h. The equilibrium adsorption data were best described by the BS adsorption isotherm model. The BS and Langmuir maximum adsorption capacities of 368.0 and 352.3 mg/g were obtained, respectively, which are high when compared with activated carbon from other precursors. The adsorption kinetics was found to follow the Avrami model platform. Adsorption of 2,4-D on CSAC was influenced by initial solution pH showing that the adsorption was characterized by interaction between 2,4-D molecules and the CSAC surface. Generally, CSAC showed excellent adsorptive characteristics and could be used as a good adsorbent for the removal of 2,4-D from water.

Acknowledgments

The first author acknowledges the award of USM-TWAS postdoctoral fellowship in aid for research. Support of Deanship of Scientific Research grant for Research Groups RGP-VPP-292 at King Saud University is appreciated by M. Asif.

References

[1] A. Zapata, I. Oller, C. Sirtori, A. Rodríguez, J.A. Sánchez-Pérez, A. López, M. Mezcua, S. Malato, Decontamination of industrial wastewater containing pesticides by combining large-scale homogeneous solar photocatalysis and biological treatment, Chem. Eng. J. 160 (2010) 447–456.

[2] S. Navarro, J. Fenoll, N. Vela, E. Ruiz, G. Navarro, Removal of ten pesticides from leaching water at pilot plant scale by photo-Fenton treatment, Chem. Eng. J. 167 (2011) 42–49.

[3] A. Derylo-Marczewska, M. Blachnio, A.W. Marczewski, A. Swiatkowski, B. Tarasiuk, Adsorption of selected herbicides from aqueous solutions on activated carbon, J. Therm. Anal. Calorim. 101 (2010) 785–794.

[4] Z. Al-Qodah, A.T. Shawaqfeh, W.K. Lafi, Adsorption of pesticides from aqueous solutions using oil shale ash, Desalination 208 (2007) 294–305.

[5] A. Addoun, W. Bencheikh, L. Temdrara, M. Belhachemi, A. Khelifi, Adsorption behavior of phenol on activated carbons prepared from Algerian coals, Desalin. Water Treat. 52 (2014) 1674–1682.

[6] L. Huang, M. Wang, C. Shi, J. Huang, B. Zhang, Adsorption of tetracycline and ciprofloxacin on activated carbon prepared from lignin with H_3PO_4 activation, Desalin. Water Treat. 52 (2014) 2678–2687.

[7] J. Kong, L. Huanga, Q. Yue, B. Gaoa, Preparation of activated carbon derived from leather waste by H_3PO_4 activation and its application for basic fuchsin adsorption, Desalin. Water Treat. 52 (2014) 2440–2449.

[8] K. Pirzadeha, A.A. Ghoreyshia, Phenol removal from aqueous phase by adsorption on activated carbon prepared from paper mill sludge, Desalin. Water Treat. (2013). doi:10.1080/19443994.2013.821034.

[9] Y. Zhang, X.-L. Song, S.-T. Huang, B.-Y. Geng, C.-H. Chang, I.-Y. Sung, Adsorption of nitrate ions onto activated carbon prepared from rice husk by NaOH activation, Desalin. Water Treat. (2013), doi:10.1080/19443994.2013.809984.

[10] K. Belarouia, A. Seghiera, M. Hadjela, Synthesis of activated carbon based on apricot stones for wastewater treatment, Desalin. Water Treat. 52 (2014) 1422–1433.

[11] V.K. Gupta, I. Ali, V.K. Saini, Adsorption of 2,4-D and carbofuran pesticides using fertilizer and steel industry wastes, J. Colloid Interface Sci. 299 (2006) 556–563.

[12] Y. Xi, M. Mallavarapu, R. Naidu, Adsorption of the herbicide 2,4-D on organo-palygorskite, Appl. Clay Sci. 49 (2010) 255–261.

[13] N. Ayar, B. Bilgin, G. Atun, Kinetics and equilibrium studies of the herbicide 2,4-dichlorophenoxyacetic acid adsorption on bituminous shale, Chem. Eng. J. 138 (2008) 239–248.

[14] I. Pavlovic, C. Barriga, M.C. Hermosın, J. Cornejo, M.A. Ulibarri, Adsorption of acidic pesticides 2,4-D, clopyralid and picloram on calcined hydrotalcite, Appl. Clay Sci. 30 (2005) 125–133.

[15] B.K. Jung, Z. Hasan, S.H. Jhung, Adsorptive removal of 2,4-dichlorophenoxyacetic acid (2,4-D) from water with a metal–organic framework, Chem. Eng. J. 234 (2013) 99–105.

[16] H.-Y. Kim, S.-N. Kim, J. Kim, W.-S. Ahn, Liquid phase adsorption of selected chloroaromatic compounds over metal organic frameworks, Mater. Res. Bull. 48 (2013) 4499–4505.

[17] J. Yang, K. Qiu, Preparation of activated carbons from walnut shells via vacuum chemical activation and their application for methylene blue removal, Chem. Eng. J. 165 (2010) 209–217.

[18] V.O. Njoku, K.Y. Foo, B.H. Hameed, Microwave-assisted preparation of pumpkin seed hull activated carbon and its application for the adsorptive removal of 2,4-dichlorophenoxyacetic acid, Chem. Eng. J. 215–216 (2013) 383–388.

[19] E.M. Ayan, A. Toptas, G. Kibrislioglu, E.E.S. Yalcinkaya, J. Yanik, Biosorption of dyes by natural and activated vine stem. Interaction between biosorbent and dye, Clean – Soil, Air, Water 39 (2011) 406–412.

[20] A.A. Halim, H.A. Aziz, M.A.M. Johari, K.S. Ariffin, Comparison study of ammonia and COD adsorption on zeolite, activated carbon and composite materials in landfill leachate treatment, Desalination 262 (2010) 31–35.

[21] J. Cao, Y. Wu, Y. Jin, P. Yilihan, S. Yang, Dynamic adsorption of anionic dyes by apricot shell activated carbon, Desalin. Water Treat. (2013). doi:10.1080/19443994.2013.871349.

[22] V.O. Njoku, B.H. Hameed, Preparation and characterization of activated carbon from corncob by chemical activation with H_3PO_4 for 2,4-dichlorophenoxyacetic acid adsorption, Chem. Eng. J. 173 (2011) 391–399.

[23] A. Jusoh, S.S. Lam, W.J.H. Hartini, N. Ali, Removal of pesticide in agricultural runoff using granular-activated carbon: A simulation study using a fixed-bed column approach, Desalin. Water Treat. 52 (2014) 861–866.

[24] A.A. Ahmad, A. Idris, B.H. Hameed, Modeling of disperse dye adsorption onto bamboo-based activated carbon in fixed-bed column, Desalin. Water Treat. 52 (2014) 248–256.

[25] L. Temdrara, A. Addoun, A. Khelifi, Development of olive stones-activated carbons by physical, chemical and physicochemical methods for phenol removal: A comparative study, Desalin. Water Treat. (2013). doi:10.1080/19443994.2013.838523.

[26] J.M. Salman, V.O. Njoku, B.H. Hameed, Bentazon and carbofuran adsorption onto date seed activated carbon: Kinetics and equilibrium, Chem. Eng. J. 173 (2011) 361–368.

[27] P. Chingombe, B. Saha, R.J. Wakeman, Effect of surface modification of an engineered activated carbon on the sorption of 2,4-dichlorophenoxy acetic acid and benazolin from water, J. Colloid Interface Sci. 297 (2006) 434–442.

[28] J.M. Salman, B.H. Hameed, Adsorption of 2,4-dichlorophenoxyacetic acid and carbofuran pesticides onto granular activated carbon, Desalination 256 (2010) 129–135.

[29] S.D. Faust, O.M. Aly, Chemistry of Water Treatment, Lewis Publishers, Boca Raton, FL, 1998.

[30] H. Marsh, F. Rodríguez-Reinoso, Activated Carbon, Elsevier, Oxford, 2006.

[31] H. Dolas, O. Sahin, C. Saka, H. Demir, A new method on producing high surface area activated carbon: The effect of salt on the surface area and the pore size distribution of activated carbon prepared from pistachio shell, Chem. Eng. J. 166 (2011) 191–197.

[32] J. Bu, G. Loh, C.G. Gwie, S. Dewiyanti, M. Tasrif, A. Borgna, Desulfurization of diesel fuels by selective adsorption on activated carbons: Competitive adsorption of polycyclic aromatic sulfur heterocycles and polycyclic aromatic hydrocarbons, Chem. Eng. J. 166 (2011) 207–217.

[33] IUPAC, IUPAC manual of symbols and terminology, Pure Appl. Chem. 31 (1972) 578–638.

[34] V. Mishra, C. Balomajumder, V.K. Agarwal, Zn(II) ion biosorption onto surface of eucalyptus leaf biomass: Isotherm, kinetic, and mechanistic modeling, Clean – Soil, Air, Water 38 (2010) 1062–1073.

[35] A.A. Ahmad, B.H. Hameed, Reduction of COD and color of dyeing effluent from a cotton textile mill by adsorption onto bamboo-based activated carbon, J. Hazard. Mater. 172 (2009) 1538–1543.

[36] D. Prahas, Y. Kartika, N. Indraswati, S. Ismadji, Activated carbon from jackfruit peel waste by H_3PO_4 chemical activation: Pore structure and surface chemistry characterization, Chem. Eng. J. 140 (2008) 32–42.

[37] J.M.V. Nabais, C.E.C. Laginhas, P.J.M. Carrott, M.M.L.R. Carrott, Production of activated carbons from almond shell, Fuel Process. Technol. 92 (2011) 234–240.

[38] A. El-Nemr, O. Abdelwahab, A. El-Sikaily, A. Khaled, Removal of direct blue-86 from aqueous solution by new activated carbon developed from orange peel, J. Hazard. Mater. 161 (2009) 102–110.

[39] I. Langmuir, The adsorption of gases on plane surfaces of glass, mica and platinum, J. Am. Chem. Soc. 40 (1918) 1361–1403.

[40] S. Kumagai, H. Ishizawa, Y. Toida, Influence of solvent type on dibenzothiophene adsorption onto activated carbon fiber and granular coconut-shell activated carbon, Fuel 89 (2010) 365–371.

[41] H. Freundlich, Über die adsorption in lösungen [Adsorption in solution], Z. Phys. Chem. 57 (1906) 384–470.

[42] W. Gu, C. Sun, Q. Liu, H. Cui, Adsorption of avermectins on activated carbon: Equilibrium, kinetics, and UV-shielding, Trans. Nonferrous Met. Soc. China 19 (2009) s845–s850.

[43] M.J. Temkin, V. Pyzhev, Recent modifications to Langmuir isotherms, Acta Physiochim. USSR 12 (1940) 217–222.

[44] R. Baccar, P. Blánquez, J. Bouzid, M. Feki, M. Sarrà, Equilibrium, thermodynamic and kinetic studies on adsorption of commercial dye by activated carbon derived from olive-waste cakes, Chem. Eng. J. 165 (2010) 457–464.

[45] F. Brouers, O. Sotolongo, F. Marquez, J.P. Pirard, Microporous and heterogeneous surface adsorption isotherms arising from levy distributions, Physica A 349 (2005) 271–282.

[46] M.J. Warrens, On similarity coefficients for 2×2 tables and correction for chance, Psychometrika 73 (2008) 487–502.

[47] B.M. Steece, The relationship of the corrected coefficient of determination and the partial F-statistics, Trabajos de Estadística y de Investigación Operativa 27 (2008) 269–273.

[48] M.C. Ncibi, S. Altenor, M. Seffen, F. Brouers, S. Gaspard, Modelling single compound adsorption onto porous and non-porous sorbents using a deformed Weibull exponential isotherm, Chem. Eng. J. 145 (2008) 196–202.

[49] K.R. Hall, L.C. Eagleton, A. Acrivos, T. Vermeulen, Pore- and solid-diffusion kinetics in fixed-bed adsorption under constant-pattern conditions, Ind. Eng. Chem. Fundam. 5 (1966) 212–223.

[50] F.W. Shaarani, B.H. Hameed, Batch adsorption of 2,4-dichlorophenol onto activated carbon derived from agricultural waste, Desalination 255 (2010) 159–164.

[51] B.H. Hameed, J.M. Salman, A.L. Ahmad, Adsorption isotherm and kinetic modeling of 2,4-D pesticide on activated carbon derived from date stones, J. Hazard. Mater. 163 (2009) 121–126.

[52] S. Lagergren, Zur theorie der sogenannten adsorption geloester stoffe [About the theory of so-called adsorption of soluble substances], Kungliga Svenska Vetenskapsakad, Handlingar 24 (1898) 1–39.

[53] Y.S. Ho, G. McKay, Pseudo-second-order model for sorption processes, Process Biochem. 34 (1999) 451–465.

[54] M.J.D. Low, Kinetics of chemisorption of gases on solids, Chem. Rev. 60 (1960) 267–312.

[55] A.M.M. Vargas, A.L. Cazetta, M.H. Kunita, T.L. Silva, V.C. Almeida, Adsorption of methylene blue on activated carbon produced from flamboyant pods (*Delonix regia*): Study of adsorption isotherms and kinetic models, Chem. Eng. J. 168 (2011) 722–730.

[56] E.C.N. Lopes, F.S.C. dos Anjos, E.F.S. Vieira, A.R. Cestari, An alternative Avrami equation to evaluate kinetic parameters of the interaction of Hg(II) with thin chitosan membranes, J. Colloid Interface Sci. 263 (2003) 542–547.